The Effect of Antinotches on Domain Wall Mobility in Single Crystal Ferroelectric Nanowires

McQuaid, R. G. P., Chang, L-W., & Gregg, M. (2010). The Effect of Antinotches on Domain Wall Mobility in Single Crystal Ferroelectric Nanowires. Nano Letters, 10(9), 3566-3571. DOI: 10.1021/nl101830d

Published in:
Nano Letters

NANO LETTERS

pubs.acs.org/NanoLett

The Effect of Antinotches on Domain Wall Mobility in Single Crystal Ferroelectric Nanowires

R. G. P. McQuaid, L.-W. Chang, and J. M. Gregg*

Centre for Nanostructured Media, School of Maths and Physics, Queen's University Belfast, Belfast, BT7 1NN, U.K.

ABSTRACT Changes in domain wall mobility, caused by the presence of antinotches in single crystal $BaTiO_3$ nanowires, have been investigated. While antinotches appeared to cause a slight broadening in the distribution of switching events, observed as a function of applied electric field (inferred from capacitance–voltage measurements), the effect was often subtle. Greater clarity of information was obtained from Rayleigh analysis of the capacitance variation with ac field amplitude. Here the magnitude of the domain wall mobility parameter (α) associated with irreversible wall movements was found to be reduced by the presence of antinotches—an effect which became more noticeable on heating toward the Curie temperature. The reduction in this domain wall mobility was contrasted with the noticeable enhancement found previously in ferroelectric wires with *notches*. Finite element modeling of the electric field, developed in the nanowires during switching, revealed regions of increased and decreased local field at the center of the notch and antinotch structures, respectively; the absolute magnitude of field enhancement in the notch centers was considerably greater than the field reduction in the center of the antinotches and this was commensurate with the manner in, and degree to, which domain wall mobility appeared to be affected. We therefore conclude that the main mechanism by which morphology alters the irreversible component of the domain wall mobility in ferroelectric wire structures is via the manner in which morphological variations alter the spatial distribution of the electric field.

KEYWORDS ferroelectrics, domains, nanowires, switching, notches, domain walls

In the last 10 years there has been a surge of activity to develop complete control over the manner in which magnetic domain walls move through nanostructured materials. This new science has been seen as critical for creating revolutionary new computational technologies, such as the "race-track" memory suggested by Parkin and co-workers.[1] While no commercially available devices have yet been developed, a variety of sophisticated ways in which domain wall propagation can be started or stopped has been demonstrated: both conventional externally applied magnetic field and the more unusual current-mediated momentum transfer, associated with electron spin flipping across domain walls, have been used to drive domain wall motion;[1−7] equally, perturbations in surface morphology[1,8] and highly localized flux-coupling techniques[9,10] have been used to stop domain walls and fix their positions.

In the midst of this *ferromagnetic* research activity, the science associated with domain wall propagation and control, within nanostructures of the analogous *ferroelectric* ferroic subgroup, has been almost completely overlooked. Basic research on the functional characteristics of ferroelectric nanowires is at a relatively embryonic stage,[11−18] and only one study has been done to date to investigate the effects of surface notches on switching.[19] While ferroelectric race tracks are not proposed to be of any immediate technological interest, basic mapping of the manner in which domain walls migrate in small scale ferroelectric objects is nevertheless highly important for applications, as switching of smaller and more morphologically complex capacitors will be needed in future ferroelectric random access memory (FeRAM) chips,[20] if road maps are adhered to.

In this Letter, we present electrical data in which the characteristics of ferroelectric nanowires with surface antinotch perturbations are compared to those of simple wire morphology. By examining ferroelectric switching, and by using Rayleigh analysis of low field capacitance behavior, we conclude that antinotches inhibit the propagation of domain walls. We suspect that this reduced domain wall mobility does not occur because of any direct pinning interaction but is rather a result of the manner in which the antinotch alters the magnitude of the electric field experienced locally by the domain walls as they sweep along the length of the wire.

The single crystal wire structures used in this study were machined from commercially obtained bulk $BaTiO_3$, using a single beam FEI200TEM focused ion beam microscope (FIB). Initially, FIB-milled lamellae (∼300 nm in thickness, and ∼6×10 μm^2) were transferred from the host bulk crystal from which they had been cut onto functionally passive MgO single crystal carriers and then incorporated into capacitor structures using coplanar Pt electrodes, as reported in previous investigations.[19,21,22] Additional FIB patterning of the $BaTiO_3$, within the interelectrode gap, allowed a pair of wires ∼2 μm in length and ∼900 nm in

* email: m.gregg@qub.ac.uk.
Received for review: 05/24/2010
Published on Web: 08/17/2010

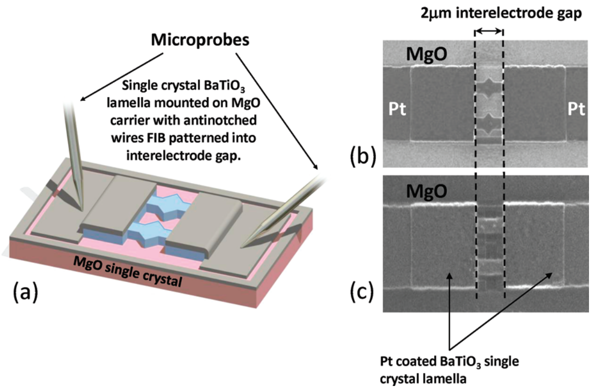

FIGURE 1. (a) Schematic representation of the capacitor test structure used to investigate how antinotches alter axial switching behavior of ferroelectric nanowires. Plan view secondary electron images of a $BaTiO_3$ lamella mounted on MgO with coplanar electrodes are also included, wherein (b) antinotched wires have been machined in the interelectrode gap and (c) the antinotches have been milled away leaving a simple wire morphology.

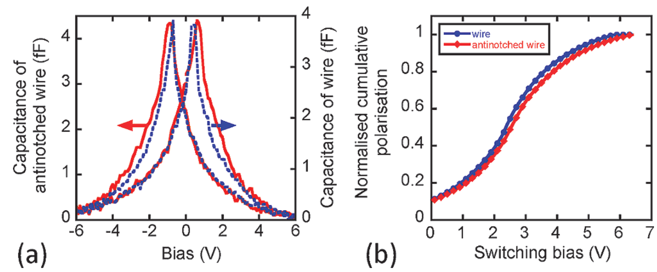

FIGURE 2. Capacitance as a function of dc bias (CV) applied axially along single crystal $BaTiO_3$ nanowires both with an antinotch at their midpoint and after the antinotch has been removed, leaving a plain wire structure. In both cases, only the change in capacitance across the switching cycle is shown; hence zero capacitance values have been arbitrarily assigned to the fully switched states. The CV response for antinotched wires clearly shows a more diffuse switching profile, with respect to applied bias, than for wires. (b) The CV data were used to numerically reconstruct the manner in which the polarization developed during a full switching cycle. Only a single branch of the reconstructed loop is shown, in each case, for clarity. The normalized polarization-development-profile maps voltage switching between the two oppositely poled final states. Polarization development is compared for profiles after 10% backswitching had already occurred, as the determination of the exact point at which the initiation of backswitching occurs from CV profiles was somewhat subjective.

width, with triangular protrusions (antinotches) close to their midpoint, to be defined. These structures are shown schematically in Figure 1a and in the plan-view secondary electron image shown in Figure 1b. Annealing in air at elevated temperatures (700 °C) enabled damaged amorphous surface regions, associated with the FIB processing, to be fully recrystallized and gallium to be simultaneously flushed out of the nanostructured specimen.[21−23] Electrical measurements were then performed to allow the switching characteristics, as well as the domain wall mobility, to be mapped. Further FIB patterning was used to remove the antinotch protrusions, yielding simple wire structures (the plan-view secondary electron image is shown in Figure 1c); after an additional thermal anneal, further electrical testing was performed to allow comparisons between domain wall dynamics in plain wire structures and those with antinotches to be made. Importantly, reports by Chang et al.[21,22] of FIB milled single crystal $BaTiO_3$ lamellae displaying an essentially bulklike electrical response indicates that the electrical characteristics of the bulk single crystal are fully recovered by the thermal anneal stage. Meaningful comparisons between the electrical responses of antinotched and plain wires, fabricated via this processing route, are therefore possible with differences attributable to the change in morphology.

CV (capacitance as a function of applied dc voltage) switching measurements for wires, both with and without antinotches, are shown in Figure 2a. In cases where obvious differences were evident, antinotches were always associated with more diffuse switching profiles than those seen in plain wires, indicating reduced switchability. In addition, integrated CV data were used to reconstruct the manner in which overall polarization developed during a switching cycle, as a function of the change in bias applied during the switching process (Figure 2b). Due to the sensitivity of the reconstruction to the bias value at which backswitching is taken to begin, we compared the manner in which switching proceeded after 10% of the polarization had been reversed. As can be seen from Figure 2b, the difference in the switching profile is subtle, but it is nonetheless clear that the antinoch lags the wire in total switched polarization fraction across the bias range. Often, however, the degree to which antinotches broadened the CV switching characteristics was even more subtle. In such cases, we employed Rayleigh analysis of the capacitance as a function of ac field amplitude, in order to specifically probe the domain wall mobilities within the nanowire structures: while measured CV data incorporates contributions from both intrinsic lattice polarizability and domain switching, Rayleigh analysis permits the irreversible contribution from domain wall motion to be analyzed explicitly. Although originally formulated for ferromagnetic materials,[24] Rayleigh's law can be analogously expressed for ferroelectrics and used to probe the role of domain wall contributions to both the dielectric[25] and extrinsic piezoelectric responses.[26] In the Rayleigh description of the dielectric response, the permittivity ε can be described by a linear relation in field amplitude E_0[25] under the influence of a weak (subcoercive) ac exciting field ($E = E_0 \sin \omega t$)

$$\varepsilon = \varepsilon_i + \alpha E_0 \tag{1}$$

where ε_i represents the intrinsic lattice polarizability and *reversible* domain wall motion contributions (domain wall motion for which, if the field were suddenly removed, the domain walls would return to their original positions—those prior to the application of the ac field) while αE_0 represents

DOI: 10.1021/nl101830d | *Nano Lett.* **2010,** *10,* 3566–3571

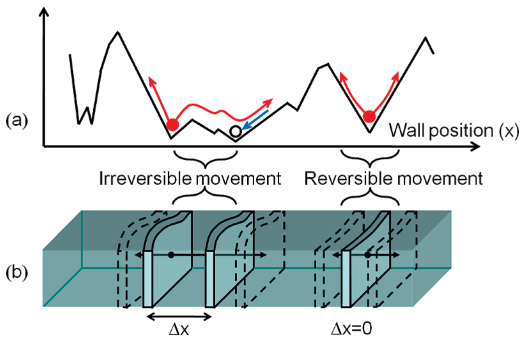

FIGURE 3. (a) A rudimentary 1D sawtooth potential profile used to envision the manner in which domain walls move through a defect-containing medium under the influence of an applied ac field. The oscillatory motions of the domain walls, within the potential landscape, are shown for the cases of reversible and irreversible displacements by red arrows. In an irreversible displacement, the domain wall can overcome its confining potential and comes to rest in a different well after field removal (indicated by the blue arrow). In a reversible displacement, the field magnitude is insufficient for the domain wall to escape and instead just oscillates within the well with a net zero displacement after field removal. (b) A graphical illustration of how this behavior would be manifested in a fictitious ferroelectric wire for two arbitrarily shaped domain walls. The dotted domain wall profiles indicate the extent of their oscillatory motion under the influence of the applied ac field.

irreversible switching contributions (domain wall motion such that, if the field were suddenly removed, the walls would be displaced from their initial positions). Re-expressing eq 1 in terms of capacitance[27]

$$C = C_i + \alpha V_0 \qquad (2)$$

where C_i is the zero-field capacitance and V_0 the amplitude of the applied ac voltage. For a review of the role of domain wall contributions to the dielectric and extrinsic piezoelectric responses of ferroelectric thin films via Rayleigh based analyses, the reader is directed to ref 28. Additionally, Kalinin and co-workers[29,30] have correlated measured Rayleigh type behavior in global dielectric data with local domain wall mobility maps obtained via PFM based techniques in polycrystalline ferroelectrics, permitting insights into the microscopic origin, and conditions for observation, of Rayleigh type behavior.

In a first attempt to provide a physical explanation for Rayleigh's law, Néel[25,31] recovered the form of eqs 1 and 2 by assuming the motion of a domain wall through a medium with a random defect distribution under weak field conditions, where the density and structure of domain walls remains unchanged.[32] The salient features of this description may be appreciated by considering the propagation of a domain wall through a rudimentary "sawtooth" potential landscape illustrated in Figure 3. Reversible polarization contributions arise when the field amplitude is insufficient for domain walls to escape their local potential minima. Instead, positional oscillations about the well minima occur.

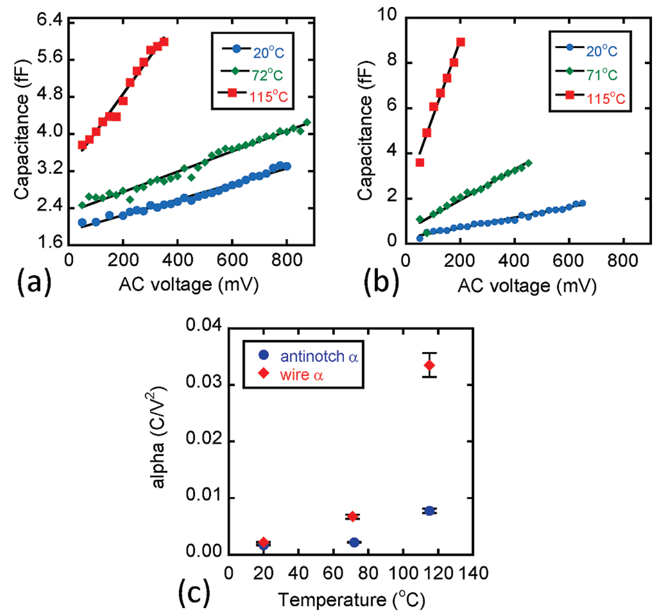

FIGURE 4. Capacitance vs ac field amplitude plots at different temperatures displayed for (a) antinotched wires and (b) straight wires in the subcoercive "Rayleigh" voltage region where data adheres to a linear trend. Best fit lines are also presented. (c) The magnitude of the gradient, α (given in units of coulombs per square volt), from each of these data sets is plotted as a function of temperature in (c) and is representative of the domain wall mobility for irreversible wall displacements in each wire geometry. Antinotches, having a smaller α, clearly reduce this domain wall mobility. This effect becomes more apparent at elevated temperatures. The uncertainties included in (c) are the standard errors from the linear regression best fit lines plotted in (a) and (b).

The polarization developed by a domain wall, during these oscillations, is proportional to its instantaneous positional displacement from the well minimum (dx). In the sawtooth picture the constant gradient of the potential as a function of position (dV/dx) is therefore commensurate with the assumed invariance of the reversible domain wall contribution to C_i (since the $C^{-1} \propto dV/dP \propto dV/dx =$ constant). Significant changes in the capacitance contributed by domain wall motion only therefore occur when the applied ac field is sufficient to allow escape from the local pinning potential minima. The increase in the capacitance with ac field amplitude therefore correlates with the irreversible domain wall motion associated with depinning and pinning during propagation. The α parameter in the Rayleigh expressions (eqs 1 and 2) is therefore a measure of mobility for irreversible domain wall motion in the presence of an applied field.

The linear regions of capacitance vs ac field amplitude for antinotched and plain wires are presented in parts a and b of Figure 4, respectively, for different temperatures. Data are omitted for field amplitudes below 50 mV (due to poor signal-to-noise) as is data beyond the voltage at which behavior becomes distinctly nonlinear. The values of the extracted irreversible components of the domain wall mobility parameters (α) are given as a function of temperature in Figure 4c. It is evident that the presence of antinotches

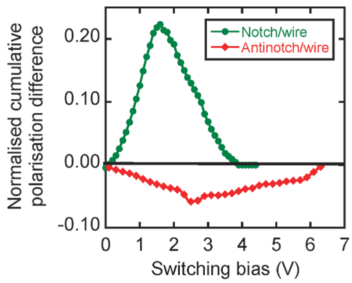

FIGURE 5. Using measured capacitance−voltage (CV) data for antinotches, plain wires, and, from previous work, notches allows the cumulative polarization developed as a function of bias voltage to be determined in each structure. Subtracting these profiles from that associated with a plain wire gives rise to the difference plots shown. These illustrate how switching is affected by the alteration in wire morphology. It is clear that notches and antinotches alter the switching profile of a simple wire in opposite senses and that the degree to which switching is enhanced by the presence of a notch is much greater in magnitude than the degree to which antinotches reduce switchability (seen by comparing peak magnitudes).

reduces the domain wall mobility and that this becomes more pronounced with increased temperature. The increasing α with temperature observed for both antinotched and plain wires is in accord with domain wall motion being a thermally activated process;[33] furthermore, this behavior is consistent with previous measurements of domain wall mobility as a function of temperature in thin films which report an increased mobility as phase transition temperatures are approached.[28,34]

Both the increased difficulty in switching antinotched ferroelectric wires (seen in CV measurements) and the overall reduced irreversible component of domain wall mobility along the wire length (seen from Rayleigh analysis) seem consistent with previous observations in magnetic nanostructures, where notches and antinotches both act as pinning centers (albeit with differing effectiveness depending on domain wall type and chirality[35,36]). Importantly, the observations also demonstrate that the increased surface area associated with features such as antinotches do not enhance switching, even though they potentially offer more boundary sites for the nucleation of reverse domains.

In previous work we observed that notched wires behaved entirely differently, enhancing ferroelectric switchability.[19] This difference in behavior prompted a closer look at the precise nature of the interactions between surface perturbations and domain walls in ferroelectrics. Figure 5 summarizes the differences in the switching characteristics of plain wires, wires with antinotches, and those with notches. Two points should be made: first, as noted above, the notches enhance switchability whereas antinotches diminish it; second, the differences between the switching characteristics of antinotch and plain wire samples is significantly more subtle than that observed between notched and plain wires.

Finite element field modeling (using Quickfield Professional) of the local field distribution along the length of the nanowires during switching (when a bias voltage is applied along the length) may give the explanation for this unusual set of observations. Figure 6a shows the local field developed, for the same overall applied bias, along the length of plain wires, wires with notches, and wires with antinotches, along with the corresponding plan-view maps of the local field from which longitudinal sections were derived (Figure 6b,c). According to these models, the local field amplitude is *reduced* through the center of the antinotch and *increased* through the center of the notch. Crucially, in addition, the absolute magnitude of the local field variation associated with the morphological perturbations was found to be considerably less for the antinotch than for the notched wires. Both of these modeled features are consistent with the domain wall dynamics and switchability measurements made experimentally and the calculated difference functions shown in figure 5.

The argument that local field modulation is primarily responsible for the observed variations in the irreversible component of domain wall mobility with surface morphology is 3-fold: first, that when compared to a simple wire, the field focusing of the notch leads to a narrowing of the voltage switching distribution; in contrast antinotch behavior, exhibiting a broader voltage switching distribution than that found in plain wires, can be explained by local dilution of

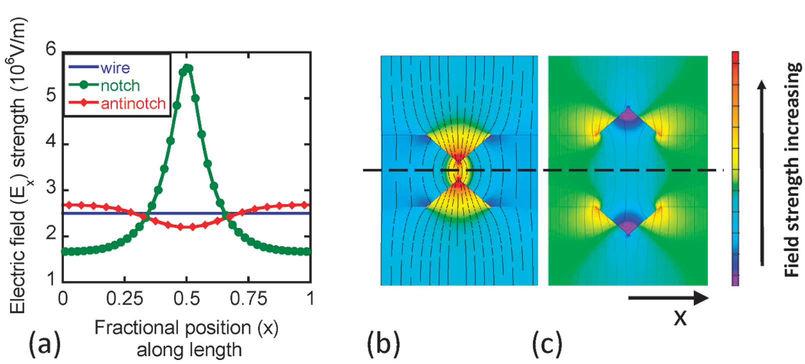

FIGURE 6. Finite element modeled variation in local electric field, when an axial bias is applied to the wires, is plotted as a function of the position along the wire axis for straight wires, notched wires, and antinotched wires. Strong field enhancement is observed through the center of a notched wire (compared to a straight wire) whereas a relatively weaker reduction in field is observed through the center of an antinotched wire. Modeled 2D maps of local field values are illustrated for notched and antinotched wires in (b) and (c), respectively. The axis along which the variation in field intensity in (a) is evaluated is indicated by the dashed line.

DOI: 10.1021/nl101830d | *Nano Lett.* **2010,** *10,* 3566--3571

the applied field; second, that the difference in voltage width of the CV switching distribution is greater for the notch/wire case than for the antinotch/wire case, commensurate with the absolute magnitudes of field variations modeled; third, that Rayleigh analysis, which permits direct insight as to how domain wall mobility is affected by the presence of the antinotch, indicates that antinotches inhibit irreversible domain wall displacements across all measured temperatures. Unlike in magnetics, where direct interaction between domain walls and engineered pinning sites is seen to occur, the current investigation strongly points to an indirect interaction in ferroelectric analogues. In the case of ferroelectrics, it appears that variations in morphology influence domain wall mobility by altering the spatial distribution of the local field during switching.

In summary, an investigation as to how antinotches affect the dynamic behavior of domain walls in patterned single crystal ferroelectric nanowires has been carried out. Both CV characterization and Rayleigh analysis indicated that antinotches reduce the irreversible component of domain wall mobility. In conjunction with previous work on notches, which were seen to enhance ferroelectric switching, and by using finite element modeling, we conclude that surface morphological perturbations affect domain wall mobility primarily by altering the local distribution of applied electric fields. That domain wall motion may be enhanced or inhibited by creating local hot or cold spots in field suggests that sample morphology could be designed to produce "field-engineered" patterns—a new concept for controlling domain dynamics in complex ferroelectric nanostructures.

Acknowledgment. The authors acknowledge financial support from the Department for Education and Learning (DEL) and the Engineering and Physical Sciences Research Council (EP/F004869/1, EP/F001630/1 and EP/H047093/1) as well as helpful discussions with J. F. Scott and G. Catalan. R.G.P.McQ. acknowledges support from the Dunville Studentship scheme.

REFERENCES AND NOTES

(1) Parkin, S. S. P.; Hayashi, M.; Thomas, L. Magnetic Domain-Wall Racetrack Memory. *Science* **2008**, *320* (5873), 190–194.
(2) Hayashi, M.; Thomas, L.; Rettner, C.; Moriya, R.; Jiang, X.; Parkin, S. S. Dependence of Current and Field Driven Depinning of Domain Walls on Their Structure and Chirality in Permalloy Nanowires. *Phys. Rev. Lett.* **2006**, *97* (20), 207205.
(3) Hayashi, M.; Thomas, L.; Rettner, C.; Moriya, R.; Parkin, S. S. P. Dynamics of domain wall depinning driven by a combination of direct and pulsed currents. *Appl. Phys. Lett.* **2008**, *92* (16), 162503.
(4) Hayashi, M.; Thomas, L.; Moriya, R.; Rettner, C.; Parkin, S. S. P. Current-Controlled Magnetic Domain-Wall Nanowire Shift Register. *Science* **2008**, *320* (5873), 209–211.
(5) Hayashi, M.; Thomas, L.; Rettner, C.; Moriya, R.; Parkin, S. S. P. Direct observation of the coherent precession of magnetic domain walls propagating along permalloy nanowires. *Nat. Phys.* **2007**, *3* (1), 21–25.
(6) Thomas, L.; Hayashi, M.; Jiang, X.; Moriya, R.; Rettner, C.; Parkin, S. S. P. Oscillatory dependence of current-driven magnetic domain wall motion on current pulse length. *Nature* **2006**, *443* (7108), 197–200.
(7) Thomas, L.; Hayashi, M.; Jiang, X.; Moriya, R.; Rettner, C.; Parkin, S. Resonant Amplification of Magnetic Domain-Wall Motion by a Train of Current Pulses. *Science* **2007**, *315* (5818), 1553–1558.
(8) Lewis, E. R.; Petit, D.; Thevenard, L.; Jausovec, A. V.; O'Brien, L.; Read, D. E.; Cowburn, R. P. Magnetic domain wall pinning by a curved conduit. *Appl. Phys. Lett.* **2009**, *95* (15), 152505.
(9) Petit, D.; Jausovec, A. V.; Zeng, H. T.; Lewis, E.; O'Brien, L.; Read, D.; Cowburn, R. P. Mechanism for domain wall pinning and potential landscape modification by artificially patterned traps in ferromagnetic nanowires. *Phys. Rev. B* **2009**, *79* (21), 214405.
(10) O'Brien, L.; Petit, D.; Zeng, H. T.; Lewis, E. R.; Sampaio, J.; Jausovec, A. V.; Read, D. E.; Cowburn, R. P. Near-Field Interaction between Domain Walls in Adjacent Permalloy Nanowires. *Phys. Rev. Lett.* **2009**, *103* (7), No. 077206.
(11) Spanier, J. E.; Kolpak, A. M.; Urban, J. J.; Grinberg, I.; Lian, O. Y.; Yun, W. S.; Rappe, A. M.; Park, H. Ferroelectric Phase Transition in Individual Single-Crystalline $BaTiO_3$ Nanowires. *Nano Lett.* **2006**, *6* (4), 735–739.
(12) Wang, Z. Y.; Suryavanshi, A. P.; Yu, M.-F. Ferroelectric and piezoelectric behaviors of individual single crystalline $BaTiO_3$ nanowire under direct axial electric biasing. *Appl. Phys. Lett.* **2006**, *89* (8), No. 082903.
(13) Wang, Z. Y.; Hu, J.; Yu, M.-F. One-dimensional ferroelectric monodomain formation in single crystalline $BaTiO_3$ nanowire. *Appl. Phys. Lett.* **2006**, *89* (8), 263119.
(14) Zhang, X. Y.; Zhao, X.; Lai, C. W.; Wang, J.; Tang, X. G.; Dai, J. Y. Synthesis and piezoresponse of highly ordered $Pb(Zr_{0.53}Ti_{0.47})O_3$ nanowire arrays. *Appl. Phys. Lett.* **2004**, *85* (18), 4190.
(15) Zhou, Z. H.; Gao, X. S.; Wang, J.; Fujihara, K.; Ramakrishna, S.; Nagarajan, V. Giant strain in $PbZr_{0.2}Ti_{0.8}O_3$ nanowires. *Appl. Phys. Lett.* **2007**, *90* (5), No. 052902.
(16) Pilania, G.; Alpay, S. P.; Ramprasad, R. Ab initio study of ferroelectricity in $BaTiO_3$ nanowires. *Phys. Rev. B* **2009**, *80* (1), No. 014113.
(17) Schilling, A.; Bowman, R. M.; Gregg, J. M.; Catalan, G.; Scott, J. F. Ferroelectric domain periodicities in nanocolumns of single crystal barium titanate. *Appl. Phys. Lett.* **2006**, *89* (21), 212902.
(18) Schilling, A.; Bowman, R. M.; Catalan, G.; Scott, J. F.; Gregg, J. M. Morphological Control of Polar Orientation in Single Crystal Ferroelectric Nanowires. *Nano Lett.* **2007**, *7* (12), 3787–3791.
(19) McMillen, M.; McQuaid, R. G. P.; Haire, S. C.; McLaughlin, C. D.; Chang, L. W.; Schilling, A.; Gregg, J. M. The influence of notches on domain dynamics in ferroelectric nanowires. *Appl. Phys. Lett.* **2010**, *96* (4), No. 042904.
(20) International Technology Roadmap for Semiconductors (ITRS), 2009 Update, 2009 Update, http://www.itrs.net/Links/2009ITRS/2009Chapters_2009Tables/2009Tables_FOCUS_C_ITRS.xls, spreadsheet title "2009_PIDS5", 2009.
(21) Chang, L.-W.; McMillen, M.; Morrison, F. D.; Scott, J. F.; Gregg, J. M. Size effects on thin film ferroelectrics: Experiments on isolated single crystal sheets. *Appl. Phys. Lett.* **2008**, *93* (13), 132904.
(22) Chang, L.-W.; Alexe, M.; Scott, J. F.; Gregg, J. M. Settling the "Dead Layer" Debate in Nanoscale Capacitors. *Adv. Mater.* **2009**, *21* (48), 4911–4914.
(23) Saad, M. M.; Bowman, R. M.; Gregg, J. M. Characteristics of single crystal "thin film" capacitor structures made using a focused ion beam microscope. *Appl. Phys. Lett.* **2004**, *84* (7), 1159–1161.
(24) Rayleigh, L. Notes on Electricity and Magnetism. III. On the Behaviour of Iron and Steel under the Operation of Feeble Magnetic Forces. *Philos. Mag.* **1887**, *23* (142), 225–245.
(25) Damjanovic, D. Stress and frequency dependence of the direct piezoelectric effect in ferroelectric ceramics. *J. Appl. Phys.* **1997**, *82* (4), 1788–1797.
(26) Damjanovic, D.; Demartin, M. The Rayleigh law in piezoelectric ceramics. *J. Phys. D: Appl. Phys.* **1996**, *29* (7), 2057–2060.
(27) Bharadwaja, S. S. N.; Moses, P. J.; Trolier-McKinstry, S.; Mayer, T. S.; Bettotti, P.; Pavesi, L. Ferroelectric and ferroelastic domain wall motion in unconstrained Pb(Zr, Ti)O_3 microtubes and thin

DOI: 10.1021/nl101830d | *Nano Lett.* **2010,** *10,* 3566–3571

films. *IEEE Trans. Ultrason. Ferroelectr. Freq. Control* **2010**, *57* (4), 792–800.
(28) Bassiri-Gharb, N.; Fujii, I.; Hong, E.; Trolier-McKinstry, S.; Taylor, D. V.; Damjanovic, D. Domain wall contributions to the properties of piezoelectric thin films. *J. Electroceram.* **2007**, *19* (1), 47–65.
(29) Seal, K.; Jesse, S.; Nikiforov, M. P.; Kalinin, S. V.; Fujii, I.; Bintachitt, P.; Trolier-Mc Kinstry, S. Spatially Resolved Spectroscopic Mapping of Polarization Reversal in Polycrystalline Ferroelectric Fims: Crossing the Resolution Barrier. *Phys. Rev. Lett.* **2009**, *103* (5), No. 057601.
(30) Bintachitt, P.; Jesse, S.; Damjanovic, D.; Han, Y.; Reaney, I. M.; Trolier-McKinstry, S.; Kalinin, S. V. Collective dynamics underpins Rayleigh behavior in disordered polycrystalline ferroelectrics. *Proc. Natl. Acad. Sci. U.S.A.* **2010**, *107* (16), 7219–7224.
(31) Neel, L. Théorie des lois d'aimantation de Lord Rayleigh. 1ere partie: les déplacements d'une paroi isolée. *Cahiers Phys.* **1942**, *12*, 1–20.
(32) Damjanovic, D. Hysteresis in Piezoelectric and Ferroelectric Materials. In *Science of Hysteresis*; Bertotti, G., Mayergoyz, I., Eds.; Elsevier: London, 2005; Vol. 3, pp 337−465.
(33) Xu, F.; Trolier-McKinstry, S.; Ren, W.; Xu, B.; Xie, Z.-L.; Hemker, K. J. Structure and piezoelectric properties of sol-gel derived (001)-oriented $Pb[Yb_{1/2}Nb_{1/2}]0_3$-$PbTiO_3$ thin films. *J. Appl. Phys.* **2001**, *89* (2), 1336–1348.
(34) Davis, D.; Damjanovic, D.; Setter, N. Temperature dependence of the direct piezoelectric effect in relaxor-ferroelectric single crystals: Intrinsic and extrinsic contributions. *J. Appl. Phys.* **2006**, *100* (8), No. 084103.
(35) Petit, D.; Jausovec, A.-V.; Read, D.; Cowburn, R. P. Domain wall pinning and potential landscapes created by constrictions and protrusions in ferromagnetic nanowires. *J. Appl. Phys.* **2008**, *103* (11), 114307.
(36) Bogart, L. K.; Atkinson, D.; O'Shea, K.; McGrouther, D.; McVitie, S. Dependence of domain wall pinning potential landscapes on domain wall chirality and pinning site geometry in planar nanowires. *Phys. Rev. B* **2009**, *79* (5), No. 054414.

DOI: 10.1021/nl101830d | *Nano Lett.* **2010,** *10,* 3566-–3571